Characterization of TiO$_2$ nanoparticle suspensions in aqueous solutions and TiO$_2$ nanoparticle retention in water-saturated columns packed with glass beads

Varvara Sygouni [a,*], Constantinos V. Chrysikopoulos [b]

[a] Environmental Engineering Laboratory, Civil Engineering Department, University of Patras, 26504 Patras, Greece
[b] School of Environmental Engineering, Technical University of Crete, 73100 Chania, Greece

HIGHLIGHTS

- We investigated the size and zeta potential of TiO$_2$ NPs suspensions.
- We conducted transport experiments of TiO$_2$ NPs in columns packed with glass beads.
- Agglomeration decreases with increasing pH and decreasing NP concentration.
- A substantial retention of the anatase TiO$_2$ NPs within the column was observed.
- Mass recovery is increasing with decreasing NP size and increasing concentration.

GRAPHICAL ABSTRACT
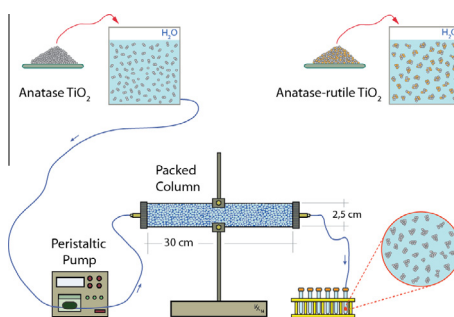
ABSTRACT

In this experimental work, various suspensions of titanium dioxide (TiO$_2$) nanoparticles (NPs) were carefully characterized, and their transport in columns packed with glass beads were thoroughly investigated. All NP suspensions were prepared with rutile–anatase and anatase TiO$_2$. Two different methods were used for the preparation of aquatic suspensions of TiO$_2$ NPs at relatively low concentrations. The average particle size and zeta potential of each suspension were estimated in order to investigate the effect of pH and sonication time on TiO$_2$ NP agglomeration. Finally, transport experiments of the various suspensions of anatase TiO$_2$ NPs were conducted. The concentration and particle size of the NPs were measured periodically at the column outlet. Also, the accumulated mass of TiO$_2$ NPs retained in the column was determined. The experimental data suggested that NP agglomeration decreases with increasing solution pH and decreasing NP concentration. Also, it was shown that a substantial percentage of the anatase TiO$_2$ NPs injected into the experimental column were retained within the column packing due to agglomeration, and that mass recovery is increasing with decreasing NP size and increasing injected concentration.

© 2014 Elsevier B.V. All rights reserved.

1. Introduction

Engineered metal oxide nanoparticles (NPs) have received considerable attention over the past few years due to their rapid large-scale production and frequent use in microelectronics, paints, catalysts, cosmetics, food, pharmaceutical industries [1–4], as well as in environmental remediation applications [5,6]. Large quantities of NPs are released into sewers, which eventually reach wastewater treatment facilities, or directly into surface waters and subsurface environment by numerous point and non-point sources, including wastewater reuse, agricultural uses, landfill

---

Nomenclature

C	concentration of NPs in suspension, M/L^3
C_o	source concentration of NPs in suspension, M/L^3
C_{max}	maximum concentration of NPs in the effluent, M/L^3
d_c	collector diameter, L
d_p	NP diameter, L
$<d_p>$	average NP diameter, L
L	length of the porous medium, L
m_o	zeroth absolute temporal moment, tM/L^3
M_a	normalized mass accumulated within the column, defined in Eq. (3), (–)
M_r	mass recovery, defined in Eq. (1), M
Q	flow rate, L^3/t
t_a	duration of aging period, t

t_p	duration of the suspension pulse, t
t_s	duration of sonication period, t

Greek Letters

ζ	electrokinetic zeta potential, V

Abbreviations

dH$_2$O	deionized water
IEP	isoelectric point
NP	nanoparticle
TiO$_2$	titanium dioxide

---

leachates, and underground storage tank leakages [7–12]. The NPs have active surfaces and can interact with molecules, organic material, biocolloids, and clays [13–15]. Consequently, NPs that enter the environment undergo surface interactions, producing very stable agglomerates, which are capable of migrating over long distances [16–24]. The toxicological risks that NPs can pose to human health and the environment have not been thoroughly examined yet [25]. To assess these potential risks, the fate and transport of NPs in environmental systems should be carefully investigated [8]. However, it should be noted that the migration behavior of NPs in subsurface formations is relatively complex [8], because it is known to be affected by many factors including solution chemistry (ionic strength, pH), temperature, flow velocity, presence of surfactants, gravity effects, and existence of biofilms [17,19,26–30]. Besides the above-mentioned environmental applications, NPs are used in Enhanced Oil Recovery for altering the interfacial tension values or contact angles in two-phase (water–oil) or three-phase flow systems (gas–water–oil) [31] or applications concerning hydraulic fracturing [32]. Also, NPs are used in medicine for functionalized bone implants [33], in photovoltaic devices [34] or memory devices [35].

Titanium dioxide (TiO$_2$) was employed in this experimental study, because it is one of the most frequently used nanomaterials in consumer products [36,6]. The stability of TiO$_2$ NPs in aqueous solutions is significantly affected by solution pH, surface charge, inorganic salts, and organic matter [13,21,23,24]. Also, the initial NP concentration plays an important role in agglomerate growth, especially for concentrations ranging between 0.1 and 10 mg/L [21]. Furthermore, the retention of TiO$_2$ NPs in porous media increases with decreasing flow rate, whereas at pH = 7 an electrostatically unfavorable condition has been reported to exist that yields maximum retention [36]. Although several studies of TiO$_2$ NP transport in porous media have assumed that NP agglomeration in porous media is negligible [17,37], when solution chemistry favors NP-NP interactions over NP–solid matrix interactions, TiO$_2$ NP agglomeration may be significant [38].

The main aim of this work is to characterize TiO$_2$ NP suspensions in aqueous solutions, and to investigate the transport of TiO$_2$ NPs with relatively low concentrations in water saturated porous media in order to improve our understanding of how agglomeration or equivalently particle size can influence NP accumulation in porous media.

2. Materials and methods

2.1. Preparation of TiO$_2$ NPs solutions

The solution pH is known to influence the NP aggregate formation [18,39]. Therefore, TiO$_2$ NP suspensions at various pH values were prepared using TiO$_2$ anatase (Aldrich 637254-50G, size < 25 nm), and TiO$_2$ anatase–rutile (Aldrich, code size < 100 nm). Two different preparation methods were applied. In the first method (M1), the TiO$_2$ NPs were first dispersed in deionized water (dH$_2$O) and then the solution pH was adjusted to the desired value. In the second method (M2), the pH of dH$_2$O was adjusted to the desired value, and then the NPs were added to the solution. In both of the preparation methods employed in this work (M1 and M2), the solution pH values were either reduced with HCl 0.1 M or increased with NaOH 0.6 M.

Sonication of NP suspensions may decrease the size of the aggregates and may yield a more stable suspension [39–42]. However, sonication is more appropriate for larger aggregates [41], and the duration of sonication should be carefully selected because excessive sonication may cause re-agglomeration of smaller particles [39,43]. In this study, TiO$_2$ suspensions were sonicated in an ultrasound bath (Elma, TI-H-5) for various time periods.

2.2. Packed columns

Flowthrough transport experiments were conducted in glass columns with 2.5-cm inner diameter and 30-cm length, which were placed horizontally to avoid gravity effects [30]. The columns were packed with glass spheres of diameter d_c = 2 mm. Each NP solution was injected into the packed column with a peristaltic pump (Masterflex, Cole Parmer). After the end of each experiment the glass spheres were cleaned carefully following the procedure suggested by Bergendahl and Grasso [44]. Briefly, the cleaning procedure consisted of washing the glass spheres with acetone, hexane and concentrated HCl, then washing the glass spheres several times with dH$_2$O, soaking them in 0.1 M NaOH solution, re-washing them several times with dH$_2$O, and drying them overnight in an oven at 105 °C. The glass column was cleaned with dense chromosulfuric acid, washed several times with dH$_2$O, and then dried in an oven.

2.3. Analytical methods

The size and zeta potential of the NPs were determined with a zeta sizer (Nano ZS90, Malvern Instruments, UK). The various NP concentrations were determined with a fluorescence spectrophotometer (Cary Eclipse, Varian Australia PTY LTD, Australia). The fluorescence spectrophotometer was equipped with a quartz cuvette (10 mm × 10 mm), and the excitation/emission wavelength was set at 625 nm [21]. It should be noted that a fluorescence spectrophotometer provides accurate measurements for liquid samples containing low concentration of scattered particles, and small particles [21,45,46].

2.4. Mass recovery and accumulation

The mass recovery, M_r [−], of the NPs injected into the packed column was quantified by the following expression [47]

$$M_r(L) = \frac{m_0(L)}{C_0 t_p} \tag{1}$$

where C_0 [M/L^3] is the source concentration of NPs suspended in the aqueous phase, t_p [t] is the broad pulse duration of the injected NPs, L [L] is the porous medium (column) length, and m_0 [tM/L^3] is the zeroth absolute temporal moment, which describes the mass of NPs in the breakthrough curve:

$$m_0(L) = \int_0^\infty C(L, t)dt \tag{2}$$

where C [M/L^3] is the concentration of NPs in suspension.

The normalized mass of the TiO$_2$ NPs injected in the column, which was accumulated within the column at time t, M_a [−] was calculated using the following equation:

$$M_a(L, t) = \frac{1}{C_0 t_p} \int_0^t [C_0 - C(L, t)]dt \tag{3}$$

3. Results and discussion

3.1. Effect of pH on TiO$_2$ NP suspensions

The particle diameters, d_p [L], and electrokinetic zeta potentials, ζ [V], of the various TiO$_2$ NP suspensions prepared in this work, with both M1 and M2 methods, were measured, listed in Table 1, and graphically presented in Fig. 1. The resulting d_p values were not sensitive to the method of preparing NP suspensions except for anatase–rutile TiO$_2$ NP suspensions at pH < 4 and pH > 10. Clearly, both methods of preparation yielded relatively similar ζ values for both anatase and rutile–anatase TiO$_2$ NP suspensions. However, the observed d_p values for anatase TiO$_2$ NP suspensions were smaller than those of rutile–anatase TiO$_2$ NP suspensions. Moreover, the ζ values of anatase TiO$_2$ NP suspensions are shown to be essentially unaffected by the solution pH. This observation
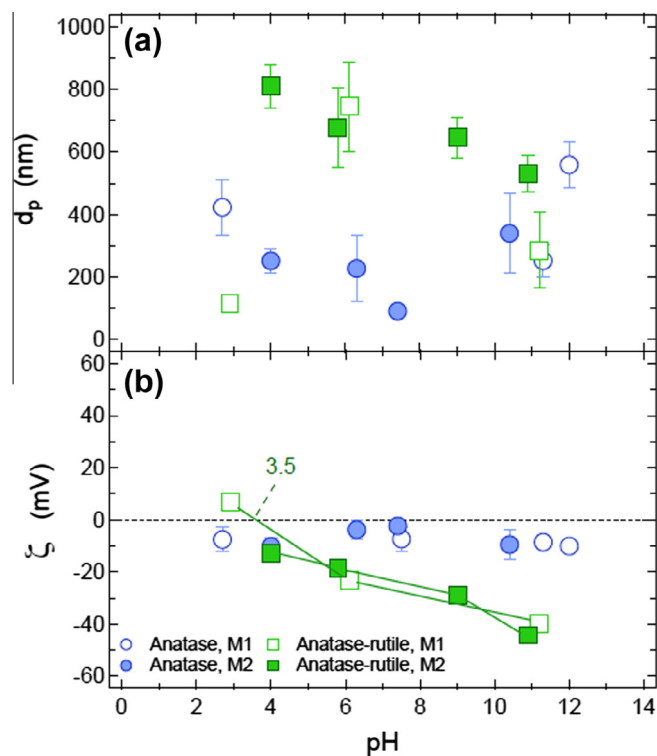
Fig. 1. Effect of solution pH on (a) particle size and (b) zeta potential of C_o = 10 mg/L anatase (circles) and C_o = 10 mg/L anatase–rutile (squares) TiO$_2$ NP suspensions, prepared by methods M1 (open symbols) and M2 (filled symbols). Also, showing is the pH$_{IEP}$ = 3.5 for anatase–rutile TiO$_2$ NP suspensions prepared with method M1. Error bars not shown are smaller than the size of the symbol.

is not in agreement with the findings presented by Fazio et al. [16] and Fang et al. [26], probably due to different initial NP concentrations and NP suspension preparation methods employed. The d_p and ζ values of anatase–rutile TiO$_2$ NP suspensions are shown in Fig. 1 to decrease with increasing pH. It should be noted that the isoelectric point (IEP), which represents the pH where the

Table 1
Zeta potential and particle size measurements.

Preparation method	pH	$\zeta \pm$ SD (mV)	$d_p \pm$ SD (nm)
TiO$_2$ anatase			
M1 no sonication (t_s = 0)	2.7	−7.6 ± 4.7	423.4 ± 90.0
	7.5	−7.4 ± 4.7	–
	11.3	−8.6 ± 2.6	252.3 ± 51.1
	12	−10.1 ± 2.6	558.7 ± 73.5
M2 no sonication (t_s = 0)	4	−10.2 ± 3.5	251.7 ± 37.5
	6.3	−3.8 ± 3.5	227.6 ± 105.7
	7.4	−2.3 ± 0.4	91.0 ± 0.8
	10.4	−9.5 ± 5.5	340.14 ± 126.7
TiO$_2$ anatase–rutile			
M1 no sonication (t_s = 0)	2.9	6.9 ± 1.5	115.8 ± 26.2
	6.1	−23.3 ± 0.85	745.7 ± 141.8
	11.2	−39.7 ± 2.9	285.5 ± 121.5
M2 no sonication (t_s = 0)	4	−12.9 ± 0.51	809.7 ± 68.3
	5.8	−18.4 ± 0.7	677.7 ± 127.2
	9	−28.7 ± 0.7	647.0 ± 65.0
	10.9	−44.2 ± 1.3	530.0 ± 57.0
M2 30 min sonication (t_s = 30 min)	4	−9.8 ± 0.8	1054.0 ± 120.4
	5.8	−29.7 ± 0.7	437.9 ± 36.6
	10.9	−42.3 ± 0.85	326.0 ± 38.0
M2 30 min sonication & 1 day aging (t_s = 30 min, t_a = 1 d)	4	−12.0 ± 1.3	811.0 ± 260.0
	5.8	−26.3 ± 0.5	417.9 ± 3.4
	10.9	−41.5 ± 0.8	267.0 ± 61.5

electrophoretic mobility changes from positive to negative, for anatase–rutile suspensions prepared by the M1 method, was found to be equal to $pH_{IEP} = 3.5$ (see Fig. 1b). A similar pH_{IEP} has also been reported in the literature for a rutile TiO_2 NP suspension [48]. However, depending on the manufacturer, pH_{IEP} values for TiO_2 NP suspensions can vary considerably [48,49]. The ζ values for anatase–rutile TiO_2 NP suspensions prepared by the M2 method, and for anatase TiO_2 NP suspensions prepared by both M1 and M2 methods, were negative for all pH values examined in this study (see Fig. 1b); but the possibility of switching to positive ζ values at lower pH values cannot be ruled out.

Relatively small, suspended particles, with high absolute ζ values are expected to exhibit better stability than suspended particles with low absolute ζ values. At low absolute ζ values, aggregates are formed because attracting forces between suspended particles are stronger than repulsive forces [26,50–52]. For the pH range examined in this work, anatase TiO_2 NP suspensions, formed smaller aggregates than anatase–rutile TiO_2 NP suspensions; however, the anatase TiO_2 NP suspensions exhibited smaller absolute ζ values than anatase–rutile TiO_2 NP suspensions.

3.2. Effect of sonication time

Sonication of suspended particles is known to reduce the size of aggregates, and also to provide relatively stable suspensions [39–42]. To obtain the optimum sonication period, t_s [t], several concentrations of anatase–rutile NP suspensions, prepared by method M2 at pH = 7 were sonicated for varying time periods, as shown in Figs. 2a and 3. Clearly, the results suggest that the mean d_p of NP suspensions without sonication ($t_s = 0$) and with sonication ($t_s > 0$) increases with increasing initial NP concentration. This result is consistent with the observations made by Brunelli et al. [21] who reported that the initial TiO_2 NP concentration plays a
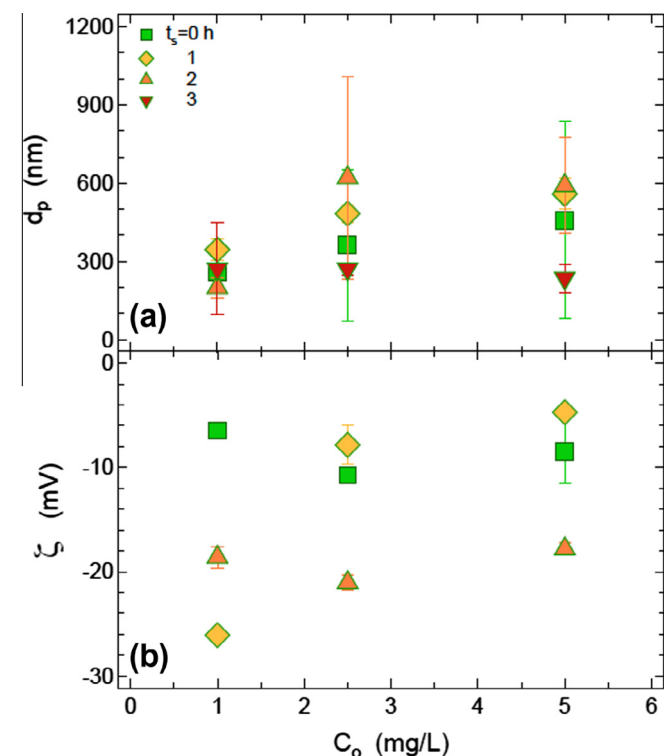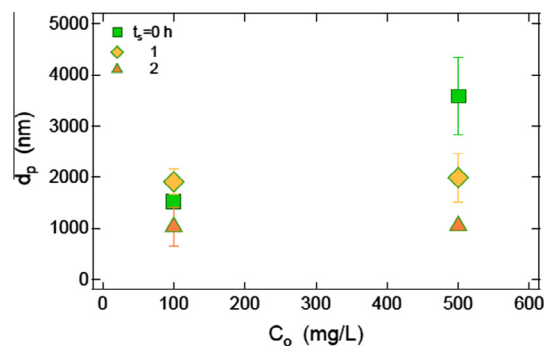
Fig. 3. Effect of sonication time on particle size of anatase–rutile TiO_2 NP suspensions prepared with method M2, at two relatively high initial concentrations. Error bars not shown are smaller than the size of the symbol.

key role on NP agglomeration and sedimentation in aquatic solutions, whereas other parameters (e.g., ionic strength, salt content and dissolved organic carbon) are of less importance. However, it should be noted, for relatively small initial concentrations ($C_o \leqslant 5$ mg/L), the range of d_p values observed for $t_s = 2$ h is much greater than that for $t_s = 1$ h and 3 h (see Fig. 2a). For relatively high initial concentrations ($C_o \geqslant 500$ mg/L), the time period of sonication plays an important role because the mean d_p, as well as its range decreases with increasing t_s (see Fig. 3). These observations are in agreement with the results presented by Horst et al. [39] and Jiang et al. [41] who noted that sonication is appropriate for the breakage of large agglomerates, but it is not effective for the small sizes, because extended sonication may cause re-agglomeration due to increased collision frequency of smaller particles. The data presented in Fig. 2b suggest that there is no clear trend between the measured ζ values and t_s as a function of C_o.

Anatase–rutile TiO_2 NP suspensions with $C_o = 10$ mg/L, prepared by method M2 at various pH values, were also sonicated for $t_s = 30$ min. The d_p and ζ values of the NP suspensions were measured immediately after sonication, and once again after a time delay or aging time, t_a [t], of one day ($t_a = 1$ d). The experimental results are graphically illustrated in Fig. 4, and suggest that with or without sonication and aging, d_p and ζ decreased with increasing solution pH. Worthy to note is that at pH > 6, d_p decreased with sonication compared to the case of no sonication, and decreased more with aging (see Fig. 4a). Also, at pH ~ 6, ζ became more negative (more stable) with sonication, and even more negative with aging; whereas, at pH ~ 6, sonication and aging did not significantly affect ζ. Consequently, a short time of sonication ($t_s \sim 30$ min) at pH > 6 are considered optimum conditions for anatase–rutile TiO_2 NP suspensions.

3.3. Transport experiments

All transport experiments were conducted with anatase TiO_2 NP suspensions prepared by method M2 at pH = 7, without sonication and aging ($t_a = t_s = 0$). Note that at pH = 7, anatase TiO_2 NP suspensions exhibit relatively small initial d_p (see Fig. 1a) and thus straining may not be significant, but the measured ζ values at pH = 7 suggest that anatase TiO_2 NP suspensions are more prone to agglomeration than anatase–rutile TiO_2 NP suspensions (see Fig. 1b). Three different concentrations of anatase TiO_2 NP suspensions were used in this study: $C_o = 2.5$, 5, and 7 mg/L. For each transport experiment a TiO_2 NP suspension solution was injected into the packed column with a flow rate of $Q = 2$ mL/min. When the effluent NP concentration reached a plateau, the TiO_2 NP suspension solution was replaced with dH_2O. The injection period, t_p [t], of the NP suspension was recorded and listed in Table 2. Efflu-

Fig. 2. Effect of sonication time on: (a) particle size, and (b) zeta potential of anatase–rutile TiO_2 NP suspensions prepared with method M2, as a function of initial NP concentration. Error bars not shown are smaller than the size of the symbol.
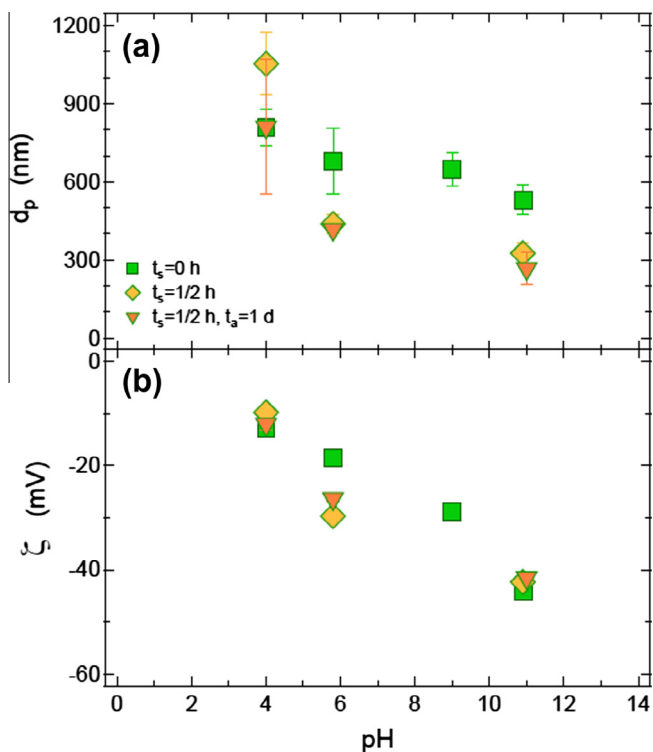
Fig. 4. Effect of solution pH on (a) particle size and (b) zeta potential of C_o = 10 mg/L anatase–rutile TiO_2 suspensions, prepared by method M2 without sonication (t_s = 0, squares), with t_s = 30 min (diamonds), and with t_s = 30 min followed by one day aging (t_a = 1 d, triangles). Error bars not shown are smaller than the size of the symbol.

ent liquid samples were collected periodically and analyzed for TiO_2 NP concentration and d_p. The breakthrough data collected from the various experiments were presented in Fig. 5. Also, the normalized maximum (peak) NP concentration from each breakthrough data set was graphically presented in Fig. 6. Note that experiments 1–3 were conducted with C_o = 2.5 mg/L (see Fig. 5a), experiments 4–6 with C_o = 5 mg/L (see Fig. 5b), and experiments 7 and 8 with C_o = 7 mg/L (see Fig. 5c). Clearly, breakthrough data obtained from experiments conducted with identical C_o are somewhat different, especially for C_o = 5 mg/L (see Fig. 5b). This variability is attributed to randomly occurring NP agglomeration within the packed column. However, as expected, the observed peak concentrations of the various transport experiments exhibited a trend of increasing values with increasing C_o (see Fig. 6).

The measured effluent d_p values from all of the transport experiments conducted in this study are presented in Fig. 7, together with the corresponding initial d_p values of the injected NP suspensions. The effluent d_p values (see Fig. 7), as well as the mean effluent $<d_p>$ values (see Table 2) were significantly different than the
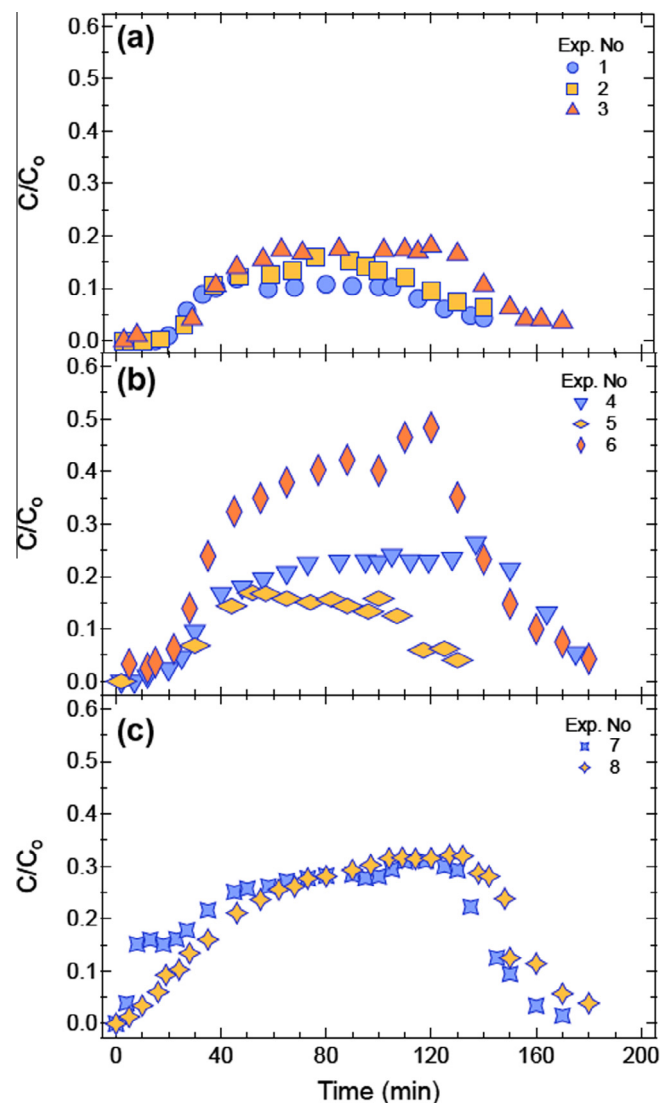
Fig. 5. Normalized effluent anatase TiO_2 NP concentration data for the transport experiments conducted with initial concentration: (a) C_o = 2.5 mg/L, (b) C_o = 5 mg/L, and (c) C_o = 7 mg/L. Here Q = 2 mL/min.

initial d_p values of the injected NP suspensions. The observed variability in the measured effluent d_p values (see Fig. 7) suggests that substantial NP agglomeration took place within the packed column during the transport experiments. This observation is in agreement with earlier work on NP agglomeration in porous media [38]. Note that there is no particular trend in the measured effluent d_p values, because there is randomness in the NP agglomeration process within the packed column. Also, effluent d_p values do not provide

Table 2
Experimental conditions and estimated M_r values.

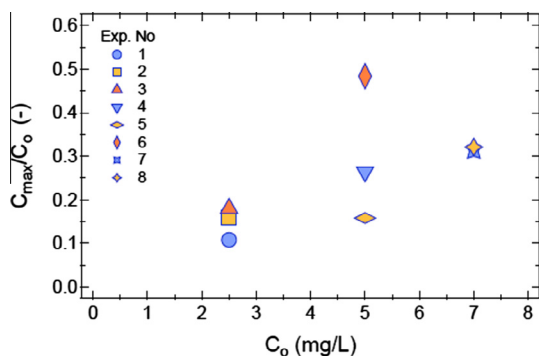| Exp. No.	C_o (mg/L)	Q (mL/min)	t_p (min)	Initial d_p (nm)	Mean effluent $<d_p>$ (nm)	M_r[a]
1	2.5	2	85	179.0	190.2	0.13
2	2.5	2	95	278.0	182.0	0.16
3	2.5	2	105	154.5	168.1	0.19
4	5	2	120	207.4	156.6	0.25
5	5	2	83	240.0	273.3	0.17
6	5	2	105	92.0	166.0	0.46
7	7	2	100	51.3	140.9	0.36
8	7	2	120	138.9	86.4	0.32

[a] Evaluated with (1).

Fig. 6. Normalized maximum effluent anatase TiO$_2$ NP concentration as a function of the injected initial TiO$_2$ NP concentration.

Fig. 8. Accumulated mass of anatase TiO$_2$ retained in the packed column of each experiment as a function of time.

a true representation of $<d_p>$ for the agglomerates formed and retained within the packed column.

The normalized mass accumulated within the packed column, M_a $[-]$, during each of the transport experiments conducted in this study was determined with Eq. (3), and presented graphically as a function of time in Fig. 8. The estimated normalized accumulated mass curve for each transport experiment was increasing linearly with time for a time period equal to t_p, and then it asymptotically
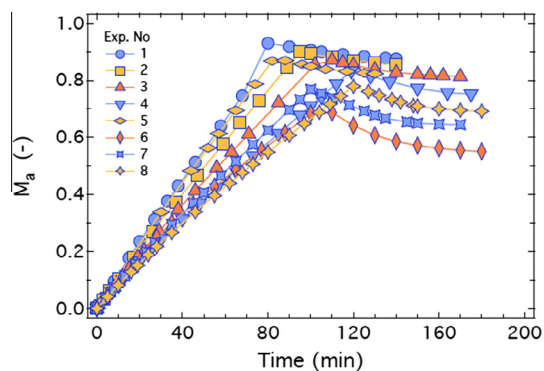
reached a plateau. The time to reach the asymptotic plateau from the maximum M_a value of each experiment was affected by NP detachment from the column solid matrix, which, as expected was more pronounced for smaller NPs. Clearly, in experiments 6–8, which were conducted with the smallest initial d_p values, more time was required for M_a to reach its asymptotic value.

The mass recovered from each of the transport experiments conducted in this study was determined with Eq. (1), listed in Table 2, and graphically illustrated in Fig. 9a, in conjunction with the corresponding initial d_p concentrations shown in Fig. 9b. Clearly, the mass recovery of the injected TiO$_2$ NPs was increasing with increasing C_o. This result is intuitive because as shown in Fig. 9b, the d_p of the injected NP suspensions was decreasing with increasing C_o. Assuming that possible agglomeration of the injected anatase TiO$_2$ NPs within the column at pH = 7 would yield particles with $d_p < 300$ nm (see Fig. 1a), then straining and wedging should
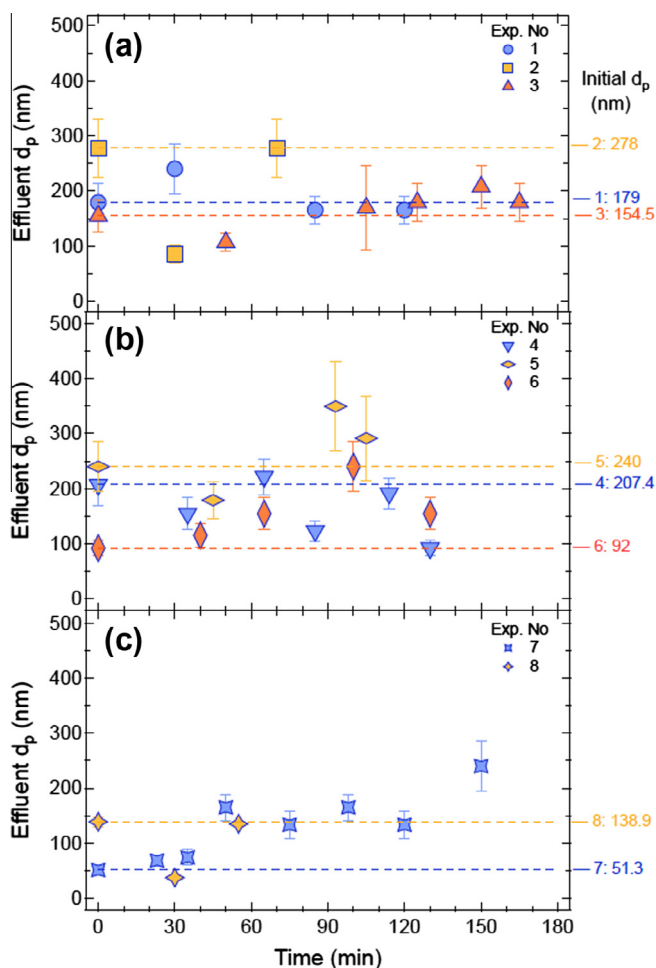

Fig. 7. Observed effluent NP sizes from transport experiments with: (a) $C_o = 2.5$ mg/L TiO$_2$, (b) $C_o = 5$ mg/L TiO$_2$, and (c) $C_o = 7$ mg/L TiO$_2$. Here $Q = 2$ mL/min. The dashed lines represent the injected initial NP sizes of the various transport experiments. Error bars not shown are smaller than the size of the symbol.
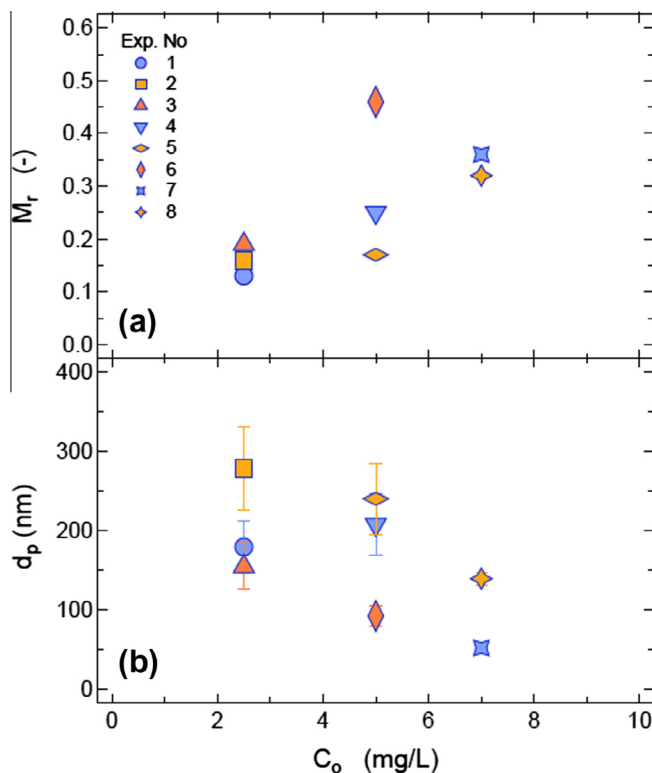

Fig. 9. Effect of initial concentration on: (a) mass recovery, as related to (b) the initial size of the injected anatase TiO$_2$ NPs.

be ruled out of possible mechanisms of mass accumulation within the packed columns examined in this study, because the corresponding colloid to collector diameter ratios ($d_p/d_c < 0.00015$) were well below the suggested threshold of 0.004 [53] or 0.003 [54]. Consequently, the observed accumulation of TiO$_2$ NPs within the column should be attributed only to physicochemical attachment processes.

4. Conclusions

The experimental results of this study revealed that smaller aggregates with smaller absolute ζ values were formed with anatase TiO$_2$ NP suspensions than anatase–rutile TiO$_2$ NP suspensions. The method of preparing NP suspensions did not significantly affect the resulting ζ values, but affected the resulting d_p values for anatase–rutile TiO$_2$ NP suspensions at pH < 4 and pH > 10. Sonication decreased the aggregate size for NP suspensions of relatively high initial concentrations, but extensive sonication could lead to re-agglomeration of low NP concentrations with small particles. Also, sonication and aging reduced NP aggregate size at relatively high pH values. The results from the transport experiments with anatase TiO$_2$ NP suspensions suggested that mass recovery of the injected TiO$_2$ NPs could increase with increasing C_o and decreasing d_p. Furthermore, NP accumulation within the packed columns was significant due to agglomeration in conjunction with physicochemical attachment rather than straining or wedging.

Acknowledgments

References

[1] F. Gottscalk, T. Sonderer, R.W. Scholz, B. Nowack, Modeled environmental concentrations of engineered nanomaterials (TiO$_2$, ZnO, Ag, CNT, fullerenes) for different regions, Environ. Sci. Technol. 43 (2009) 9216–9222.

[2] C.O. Robichaud, A.E. Uyar, M.R. Darby, L.G. Zucker, M.R. Wiesner, Estimates of upper bounds and trends in nano-TiO$_2$ production as a basis for exposure assessment, Environ. Sci. Technol. 43 (2009) 4227–4233.

[3] S.H. Kim, C.-H. Jung, N. Sahu, D. Park, J.Y. Yun, H. Ha, J.Y. Park, Catalytic activity of Au/TiO$_2$ and Pt/TiO$_2$ nanocatalysts prepared with arc plasma deposition under CO oxidation, Appl. Catal. A 454 (2013) 53–58.

[4] A. Kubacka, M.S. Diez, D. Rojo, R. Bargiela, S. Ciordia, I. Zapico, J.P. Albar, C. Barbas, V.A.P. Martins dos Santos, M. Fernandez-Garcia, M. Ferrer, Understanding the antimicrobial mechanism of TiO$_2$-based nanocomposite films in a pathogenic bacterium, Sci. Rep. 4 (2014) 4134.

[5] T. Tosco, M.P. Papini, C.C. Viggi, R. Sethi, Nanoscale zerovalent iron particles for groundwater remediation: a review, J. Clean. Prod. 77 (2014) 10–21.

[6] P.E. Neale, A.K. Jamting, B.I. Escher, J. Hermann, A review of the detection, fate and effects of engineered nanomaterials in wastewater treatment plants, Water Sci. Technol. 68 (2013) 1440–1453.

[7] M.R. Wiesner, G.V. Lowry, P. Alvarez, D. Dionysiou, P. Biswas, Assessing the risks of manufactured nanomaterials, Environ. Sci. Technol. 40 (2006) 4336–4345.

[8] S.J. Klaine, P.J.J. Alvarez, G.E. Batley, T.F. Fernandez, R.D. Handy, D.Y. Lyon, S. Mahendra, M.J. Mclaughlin, J.R. Lead, Nanomaterials in the environment: behaviour, fate, bioavailability, and effects, Environ. Toxicol. Chem. 27 (2008) 1825–1851.

[9] S.K. Brar, M. Verma, R.D. Tyagi, R.Y. Surampalli, Engineered nanoparticles in wastewater and wastewater sludge – evidence and impacts, Waste Manage. 30 (2010) 504–520.

[10] C. Botta, J. Labille, M. Auffan, D. Borschneck, H. Miche, M. Cabié, A. Masion, J. Rose, J.-Y. Bottero, TiO$_2$-based nanoparticles released in water from commercialized sunscreens in a life-cycle perspective: structures and quantities, Environ. Pollut. 159 (2011) 1543–1550.

[11] A.C. Johnson, M.J. Bowes, A. Crossley, H.P. Jarvie, K. Jurkschat, M.D. Jürgens, A.J. Lawlor, B. Park, P. Rowland, D. Spurgeon, C. Svendsen, I.P. Thompson, R.J. Barnes, R.J. Williams, N. Xu, An assessment of the fate, behaviour and environmental risk associated with sunscreen TiO$_2$ nanoparticles in UK field scenarios, Sci. Total Environ. 409 (2011) 2503–2510.

[12] J. Labille, J. Feng, C. Botta, D. Borschneck, M. Sammut, C. Martiane, M. Auffan, J. Rose, J.-Y. Bottero, Aging of TiO$_2$ nanocomposites used in sunscreen. Dispersion and fate of the degradation products in aqueous environment, Environ. Pollut. 158 (2010) 3482–3489.

[13] A.A. Keller, H. Wang, D. Zhou, H.S. Lenihan, G. Cherr, B.J. Cardinalle, R. Miller, Z. Ji, Stability and aggregation of metal oxide nanoparticles in natural aqueous matrices, Environ. Sci. Technol. 44 (2010) 1962–1967.

[14] I. Chowdhury, D.M. Cwiertny, S.L. Walker, Combined factors influencing the aggregation and deposition of nano-TiO$_2$ in the presence of humic acid and bacteria, Environ. Sci. Technol. 46 (2012) 6968–6976.

[15] L. Cai, M. Tong, X. Wang, H. Kim, Influence of clay particles on the transport and retention of titanium dioxide nanoparticles in quartz sand, Environ. Sci. Technol. 48 (2014) 7323–7332.

[16] S. Fazio, J. Guzman, M.T. Colomer, A. Salomoni, R. Moreno, Colloidal stability of nanosized titania aqueous suspensions, J. Eur. Ceram. Soc. 28 (2008) 2171–2176.

[17] J. Fang, X.-Q. Shan, B. Wen, J.-M. Lin, G. Owens, Stability of titania nanoparticles in soil suspensions and transport in saturated homogeneous soil columns, Environ. Pollut. 157 (2009) 1101–1109.

[18] R.A. French, A.R. Jacobson, B. Kim, S.L. Isley, R.L. Pen, P.C. Baveye, Influence of ionic strength, pH, and cation valence on aggregation kinetics of titanium dioxide nanoparticles, Environ. Sci. Technol. 43 (2009) 1354–1359.

[19] I.G. Godinez, C.J.G. Darnault, Aggregation and transport of nano-TiO$_2$ in saturated porous media: effects of pH, surfactants and flow velocity, Water Res. 45 (2011) 839–851.

[20] A.R. Petosa, S.J. Brennan, F. Rajput, N. Tufenkji, Transport of two metal oxide nanoparticles in saturated granular porous media: role of water chemistry and particle coating, Water Res. 46 (2012) 1273–1285.

[21] A. Brunelli, G. Pojana, S. Callegaro, A. Marcomini, Agglomeration and sedimentation of titanium dioxide nanoparticles (n-TiO$_2$) in synthetic and real waters, J. Nanopart. Res. 15 (2013) 1–10.

[22] I.G. Godinez, C.J.G. Darnault, A.P. Khodadoust, D. Bogdan, Deposition and release kinetics of nano-TiO$_2$ in saturated porous media: effects of solution ionic strength and surfactants, Environ. Pollut. 174 (2013) 106–113.

[23] M.B. Romanello, M.M. Fidalgo de Cortalezzi, An experimental study on the aggregation of TiO$_2$ nanoparticles under environmentally relevant conditions, Water Res. 47 (2013) 3887–3898.

[24] C. Xiang, Y. Feng, M. Li, M. Jaridi, N. Wu, Experimental and statistical analysis of surface charge, aggregation and adsorption behaviors of surface-functionalized titanium dioxide nanoparticles in aquatic system, J. Nanopart. Res. 15 (2013) 1293–1304.

[25] WHO, Nanotechnology and human health: Scientific evidence and risk governance, Report of the WHO expert meeting 10–11 December 2012, Bonn, Germany. Copenhagen, WHO Regional Office for Europe (2013).

[26] J. Fang, M.-J. Xu, D.-J. Wang, B. Wen, J.-Y. Han, Modeling the transport of TiO$_2$ nanoparticle aggregates in saturated and unsaturated granular media: effects of ionic strength and pH, Water Res. 47 (2013) 1399–1408.

[27] J. Rottman, R. Sierra-Alvarez, F. Shadman, Real-time monitoring of nanoparticle retention in porous media, Environ. Chem. Lett. 11 (2013) 71–76.

[28] X. Jiang, X. Wang, M. Tong, H. Kim, Initial transport and retention behaviors of ZnO nanoparticles in quartz sand porous media coated with *Escherichia coli* biofilm, Environ. Pollut. 174 (2013) 38–49.

[29] C. Kim, S. Lee, Effect of seepage velocity on the attachment efficiency of TiO$_2$ nanoparticles in porous media, J. Hazard. Mater. 279 (2014) 163–168.

[30] C.V. Chrysikopoulos, V.I. Syngouna, Effect of gravity on colloid transport through water-saturated columns packed with glass beads: modeling and experiments, Environ. Sci. Technol. 48 (2014) 6805–6813, http://dx.doi.org/10.1021/es501295n.

[31] H. ShamsiJazeyi, C.A. Miller, M.S. Wong, J.M. Tour, R. Verduzco, Polymer-coated nanoparticles for enhanced oil recovery, J. Appl. Polym. Sci. 40576 (2014) 1–13, http://dx.doi.org/10.1002/APP.40576.

[32] A. Yethiraj, A. Striolo, Fracking: what can physical chemistry offer?, J Phys. Chem. Lett. 4 (2013) 687–690.

[33] L. Li, M. Li, D. Li, P. Xe, H. Xia, Y. Zhang, C. Mao, Chemical functionalization of bone implants with nanoparticle-stabilized chitosan and methotrexate for inhibiting both osteoclastoma formation and bacterial infection, J. Mater. Chem. B 2 (36) (2014) 5952–5961.

[34] Y. Djaoued, J. Robichaud, S. Priya, B. Subramanian, E. Gondek, M. Pokladko-Kowar, P. Karasinski, I.V. Kityk, Implication of porous TiO$_2$ nanoparticles in PEDOT:PSS photovoltaic devices, high-efficiency solar cells, Springer Ser. Mater. Sci. 190 (2014) 389–447.

[35] H.Y. Jeon, J.Y. Lee, S.-Y. Choi, Interface-engineered amorphous TiO$_2$-based resistive memory devices, Adv. Funct. Mater. 20 (2010) 3912–3917.

[36] I. Chowdhury, Y. Hong, R.J. Honda, S.L. Walker, Mechanisms of TiO$_2$ nanoparticle transport in porous media: role of solution chemistry, nanoparticle concentration, and flowrate, J. Colloid Interface Sci. 360 (2011) 548–555.

[37] K.A.D. Guzman, M.P. Finnegan, J.F. Banfield, Influence of surface potential on aggregation and transport of titania nanoparticles, Environ. Sci. Technol. 40 (2006) 7688–7693.

[38] N. Solovitch, J. Labille, J. Rose, P. Chaurand, D. Borschneck, M.R. Wiesner, J.-Y. Bottero, Concurrent aggregation and deposition of TiO$_2$ nanoparticles in sandy porous media, Environ. Sci. Technol. 44 (2010) 4897–4902.

[39] A.M. Horst, Z. Ji, P.A. Holden, Nanoparticle dispersion in environmentally relevant culture media: a TiO$_2$ case study and considerations for a general approach, J. Nanopart. Res. 14 (2012) 1014.

[40] C.R. Thomas, S. George, A.M. Horst, Z. Ji, R.J. Miller, J.R. Peralta-Videa, T. Xia, S. Pokhrel, L. Madler, J.L. Gardea-Torresdey, P.A. Holden, A.A. Keller, H.S. Lenihan, A.E. Nel, J.I. Zink, Nanomaterials in the environment: from materials to high-throughput screening to the organisms, ACS Nano 5 (2011) 13–20.

[41] J. Jiang, G. Oberdorster, P. Biswas, Characterization of size, surface charge, and agglomeration state of nanoparticle dispersions for toxicological studies, J. Nanopart. Res. 11 (2009) 77–89.

[42] T.M. Sager, D.W. Porter, V.A. Robinson, W.G. Lindsley, D.E. Schwegler-Berry, V. Castranova, Improved method to disperse nanoparticles for in vitro and in vivo investigation of toxicity, Nanotoxicology 1 (2007) 118–129.

[43] I. Chowdhury, Y. Hong, S.L. Walker, Container to characterization: impacts of metal oxide handling, preparation, and solution chemistry on particle stability, Colloids Surf. A 368 (2010) 91–95.

[44] J. Bergendahl, D. Grasso, Prediction of colloid detachment in a model porous media: thermodynamics particle technology and fluidization, AIChE J. 45 (1999) 475–484.

[45] J.T.K. Quik, M.C. Stuart, M. Wouterse, W. Peijenburg, A.J. Hendrinks, D. Van De Meent, Natural Colloids are the dominant factor in the sedimentation of nanoparticles, Environ Toxicol. Chem. 31 (2012) 1019–1022.

[46] J.A. Sene, M.V.B. Pinheiro, K. Krambrock, P.J.S. Barbeira, Quantification of fullerene nanoparticles suspensions in water based on optical scattering, Talanta 78 (2009) 1503–1507.

[47] V.I. Syngouna, C.V. Chrysikopoulos, Transport of biocolloids in water saturated columns packed with sand: effect of grain size and pore water velocity, J. Contam. Hydrol. 126 (2011) 301–314, http://dx.doi.org/10.1016/j.jconhyd.2011.09.007.

[48] N. Mandzy, E. Grulke, T. Druffel, Breakage of TiO$_2$ agglomarates in electrostatically stabilized aqueous dispersion, Powder Technol. 160 (2005) 121–126.

[49] N.T. Boncagni, J.M. Otaegui, E. Warner, T. Curran, J. Ren, M.M. DeCortalezzi, Exchange of TiO$_2$ nanoparticles between streams and streambeds, Environ. Sci. Technol. 43 (2009) 7699–7705.

[50] M. Elimelech, J. Gregory, X. Jia, R.A. Williams, Particle Deposition and Aggregation: Measurement, Modeling and Simulation, Butterworth Heinemann, Oxford, UK, 1995.

[51] R. Greenwood, K. Kendall, Selection of suitable dispersants for aqueous suspensions of zirconia and titania powders using acoustophoresis, J. Eur. Ceram. Soc. 19 (1999) 479–488.

[52] D.A.H. Hanaor, M. Michelazzi, C. Leonelli, C.C. Sorrell, The effects of carboxylic acids on the aqueous dispersion and electrophoretic deposition of ZrO$_2$, J. Eur. Ceram. Soc. 32 (2012) 235–244.

[53] W.P. Johnson, E.H. Pazmino, Direct observations of colloid retention in granular media in the presence of energy barriers, and implications for inferred mechanisms from indirect observations, Water Res. 44 (2010) 1158–1169.

[54] S.A. Bradford, M. Bettahar, Concentration dependent transport of colloids in saturated porous media, J. Contam. Hydrol. 82 (2006) 99–117.